# APPLICATION OF A MODEL ADAPTIVE APPROACH TO THE SIMULATION OF DENSITY DRIVEN FLOW IN AN UNSATURATED LABORATORY SYSTEM

**Carsten THORENZ**

Leibniz Institute for Applied Geosciences
PB 510153, 30631 Hannover, GERMANY

## INTRODUCTION

The fundamentals of a numerical model for flow processes in the subsurface and a laboratory scale application example are presented. The model is part of the finite-element-method simulation package *RockFlow* (*Kolditz et al.*, 2001) and covers the simulation of saturated single-phase flow, unsaturated single-phase flow, density driven flow and multiphase flow in fractured and porous media (*Thorenz*, 2001). It is coupled to a single-phase, single-component tracer transport model to take into account for transport processes and density effects.

Due to the multitude of regarded physical processes within the flow model, a scalable approach is derived, which can treat flow processes of different complexity by up- and downsizing of a superset model. Thus, the chosen physical *model* is *adapted* to the relevant physical processes in the domain (*model adaptivity*). The downsizing methods are automatized and are suitable to adapt the underlying physical model dynamically.

Because of the lack of available benchmarks for density driven flow in partially saturated media, a laboratory scale experiment was performed. The laboratory experiments were designed according to initial simulations from the numerical model. Though the predicted behaviour of the system was quite unexpected, the experimental work proved the correctness of the prior numerical simulations. The laboratory experiment is presented together with numerical results.

## GOVERNING EQUATIONS

### Fluid mass conservation

The conservation of mass for a fluid phase $\alpha$ is regarded:

$$\frac{\partial\left(nS_\alpha\rho_\alpha\right)}{\partial t}+\operatorname{div}\left(\rho_\alpha\mathbf{q}_\alpha\right)-\rho_\alpha Q_\alpha=0 \qquad (1)$$

For this formulation it is assumed that in the REV the volumetric amount occupied by a fluid phase $\alpha$ is reduced due to porosity n and saturation $S_\alpha$. The movement of the fluid is described by the Darcy flux $\mathbf{q}_\alpha$. The production $Q_\alpha$ denotes the production in volume units per volume and time unit. For systems with negligible pressure gradients in the gaseous phase Richards' approach (*Richards*, 1930) can be used to describe saturation changes. In this case, compressibility of residual gases, water and the porous material are lumped in the specific storage coefficient $S_0$ and the saturation is described as a function of the fluid pressure:

$$\rho\left(S_0 S+n\frac{\partial S}{\partial p}\right)\frac{\partial p}{\partial t}-\operatorname{div}\left(\rho\mathbf{q}\right)-\rho Q=0 \qquad (1)$$

A modified Darcy's law is used to describe the special case of multiphase flow (*Bear* 1972, *Busch et al.* 1993, *Sahimi* 1995). The flux $\mathbf{q}_\alpha$ of phase $\alpha$ is assumed to be a non-linear function of the head gradient (expressed by the gradient of the phase pressure $p_\alpha$ and the gravitational force $\rho_\alpha \mathbf{g}$), the permeability tensor $\mathbf{k}$, the fluid viscosity $\mu$ and the relative permeability $k_{r_\alpha}$:

$$\mathbf{q}_\alpha = -\frac{k_{r_\alpha}\mathbf{k}}{\mu_\alpha}\left(\text{grad}\, p_\alpha - \rho_\alpha \mathbf{g}\right) \tag{2}$$

The changes of system variables can induce changes of the relative permeability $k_{r_\alpha}$ (due to changes of all phase saturations or non-linear behaviour because of non-negligible inertial forces), the fluid viscosity $\mu_\alpha$ and fluid density $\rho_\alpha$ (changes of fluid composition, temperature or pressure). Generally it is difficult to take care of all effects on the relative permeability in a single approach. Therefore it is supposed to treat the effects separately and to multiply all single relative permeabilities to each other, so that a total relative permeability is gained. Later this product row will be multiplied with the basic permeability tensor $\mathbf{k}$ to achieve the final permeability for a fluid phase.

The pressure field equations for multiphase flow and the Richards' equation are combined to a common equation, thus forming an equation that describes the superset of all regarded physical processes. In this equation the excessive compressibility effects must be switched on or off in respect to the desired physical behaviour.

The time derivatives of the densities are replaced by using the fluid compressibility. This simplification introduces the assumption that changes of the fluid volume are only induced by compressibility. The phase pressures are evaluated as the pressure difference between the least wetting phase (index 0) and the regarded phase (index $\alpha$). Thus, the capillary pressures $p_{c_{0,\alpha}}$, are positive and the final pressure equation with $p_0$ as primary unknown is:

$$\sum_{\alpha=0}^{\text{phases-1}}\left[\left(\frac{nS_\alpha}{\rho_\alpha}\frac{\partial \rho_\alpha}{\partial p_\alpha} + S_0 S_\alpha + n\frac{\partial S_\alpha}{\partial p_\alpha}\right)\frac{\partial\left(p_0 - p_{c_{0,\alpha}}\right)}{\partial t} - \frac{1}{\rho_\alpha}\text{div}\left(\rho_\alpha \frac{k_{r_\alpha}\mathbf{k}}{\mu_\alpha}\left(\text{grad}\, p_0 - \text{grad}\, p_{c_{0,\alpha}} - \rho_\alpha \mathbf{g}\right)\right) - Q_\alpha\right] = 0 \tag{3}$$

This equation is the "superset" pressure equation, which can be transformed to correspond to either single-phase flow of compressible or incompressible fluids, unsaturated single phase or multiphase flow by choosing the number of phases and appropriate physical parameters. By this means the chosen physical model is adapted to the needs of the modeller. This approach, called *"static model adaptivity"* in the following, was developed in order to keep the amount of redundant computer code low, as it can be reused for a large class of problems.

## Saturation field equation for multiphase flow

The mass conservation equation is converted to a volumetric one by dividing with the fluid's density. Furthermore, the assumption is introduced that the fluid volume is only influenced by changes of the pressure.

$$nS_\alpha \frac{1}{\rho_\alpha}\frac{\partial \rho_\alpha}{\partial p_\alpha}\frac{\partial p_\alpha}{\partial t} + n\frac{\partial S_\alpha}{\partial t} - \frac{1}{\rho_\alpha}\text{div}\left(\rho_\alpha \frac{k_{r_\alpha}\mathbf{k}}{\mu_\alpha}\left(\text{grad}\, p_\alpha - \rho_\alpha \mathbf{g}\right)\right) - Q_\alpha = 0 \tag{4}$$

In this equation only the first two terms contain the primary variable S, thus large parts of the equation can be treated explicitly. This is not very effective if capillary forces govern the system. In this case, the derivative of the capillary pressure function should replace the saturation in the equation.

### Governing equation for tracer transport

An advection dispersion equation (ADE) is used to model the transport process. In the ADE the motion and conservation of the concentration c of a conservative tracer $\beta$ in phase $\alpha$ is described:

$$nS_\alpha \frac{\partial c_{\alpha,\beta}}{\partial t} + q_\alpha \mathrm{div}\ c_{\alpha,\beta} - \mathrm{div}\left(nS_\alpha D_{\alpha,\beta} \mathrm{grad}\ c_{\alpha,\beta}\right) - Q_{\alpha,\beta} = 0 \qquad (5)$$

The dispersion tensor **D** is the combined molecular diffusion and hydrodynamical dispersion according to *Scheidegger* (1961).

## NUMERICAL EVALUATION

For the numerical treatment a semi-discrete Finite-Element-Method (FEM) was used. Details about the method are presented in *Thorenz* (2001). Here, only a largely simplified version is presented. To simplify the expressions, a set of matrices and vectors, which describe the sum of the element integrals of all elements, is introduced. In these matrices all spatial variables are evaluated according to their local position. The following matrices are later used to assemble the discretized form of the partial differential equations:

Pressure dependent storage: Matrix type A
Mass storage for multiphase flow: Matrix type B
Flux: Matrix type C
Gravity: Matrix type D
Sinks and sources: Matrix type E

### Model adaptive methods

The coupled systems, which are regarded here, can be described by a set of non-linear coupled partial differential equations (PDEs):

- A single pressure equation ($p_0$ unknown).
- Multiple saturation equations ($S_\alpha$ unknown).
- Multiple transport equations ($c_{\alpha,\beta}$ unknown).

These PDEs result in large systems of linear equations. Due to the non-linear coupling, these systems of linear equations have to be rebuilt multiple times in each time step, a very costly procedure. Setting up the systems of linear equations can be expensive compared to solving them. This is due to the size of the PDEs on the one hand and the advances in solver technology (BiCG solvers, preconditioners, multi grid methods etc.) on the other. The following approach has the goal to reduce the time to set up those equation systems.

#### Static a-priori adaptation of the physical model

The first step is to determine an initial physical model, which captures all effects the modeller wants to take into account. This is a very important step, as already at this point the physical system can be over- or undersized. The initial model can be assembled from the matrices mentioned in the prior chapter in a modular way. Here, the discretized matrix equations for different physical problems are presented. The variables t and t+$\Delta$t denote old and new time level, respectively:

Saturated single-phase flow of an incompressible fluid

$$\Theta \mathbf{C}_0 \mathbf{p}_0^{t+\Delta t} = -(1-\Theta)\mathbf{C}_0 \mathbf{p}_0^{t} + \mathbf{D}_0 + \mathbf{E}_0 \qquad (7)$$

Saturated single-phase flow of a compressible fluid

$$\left(\frac{1}{\Delta t}\mathbf{A}_0 + \Theta\mathbf{C}_0\right)\mathbf{p}_0^{t+\Delta t} = \frac{1}{\Delta t}\mathbf{A}_0\mathbf{p}_0^{t} - (1-\Theta)\mathbf{C}_0\mathbf{p}_0^{t} + \mathbf{D}_0 + \mathbf{E}_0 \tag{8}$$

(Un-)Saturated single-phase flow in an aquifer with storativity

$$\left(\frac{1}{\Delta t}\mathbf{A}_0 + \Theta\mathbf{C}_0\right)\mathbf{p}_0^{t+\Delta t} = \frac{1}{\Delta t}\mathbf{A}_0\mathbf{p}_0^{t} - (1-\Theta)\mathbf{C}_0\mathbf{p}_0^{t} + \mathbf{D}_0 + \mathbf{E}_0 \tag{9}$$

Multiphase flow

$$\begin{aligned}&\text{Pressure field}:\\ &\sum_{\alpha=0}^{phases-1}\left(\frac{1}{\Delta t}\mathbf{A}_\alpha + \Theta\mathbf{C}_\alpha\right)\mathbf{p}_0^{t+\Delta t} = \sum_{\alpha=0}^{phases-1}\left(\frac{1}{\Delta t}\mathbf{A}_\alpha - (1-\Theta)\mathbf{C}_\alpha\right)\mathbf{p}_0^{t} +\\ &\sum_{\alpha=0}^{phases-1}\left(\frac{1}{\Delta t}\mathbf{A}_\alpha\left(\mathbf{p}_{c_{0,\alpha}}^{t+\Delta t} - \mathbf{p}_{c_{0,\alpha}}^{t}\right)\right) + \sum_{\alpha=0}^{phases-1}\left(\mathbf{D}_\alpha + \mathbf{E}_\alpha\right)\end{aligned} \tag{10}$$

Additionally phases-1 saturation field equations must be solved after solving the pressure field equation:

$$\begin{aligned}&\text{Saturation fields}:\\ &\frac{1}{\Delta t}\mathbf{B}\,\mathbf{S}_\alpha^{t+\Delta t} = \frac{1}{\Delta t}\mathbf{B}\,\mathbf{S}_\alpha^{t} - \frac{1}{\Delta t}\mathbf{A}_\alpha\left(\mathbf{p}_0^{t+\Delta t} - \mathbf{p}_0^{t} - \mathbf{p}_{c_{0,\alpha}}^{t+\Delta t} + \mathbf{p}_{c_{0,\alpha}}^{t}\right) +\\ &-\mathbf{C}_\alpha\left(\mathbf{p}_0^{t+\Theta\Delta t} - \mathbf{p}_{c_{0,\alpha}}^{t+\Theta\Delta t}\right) + \mathbf{D}_\alpha + \mathbf{E}_\alpha\end{aligned} \tag{11}$$

## Runtime adaptation of the physical model

The PDEs to describe the movement of fluids and solutes in non-linearly coupled systems are costly to evaluate. For the pressure field, it is useful to dynamically choose a subset of the superset pressure PDE (3. This subset is valid in the entire domain.

It is obvious that the fluid mobilities for some phases may be equal to zero in parts of the domain, as the saturation of the appropriate phase can fall below the residual saturation. As a consequence it is absolutely legitimate to ignore the matrices of type **C** and **D** in the appropriate part of the domain for these phases if the saturation drops below the residual saturation. This evaluation is performed as a first step, resulting in a largely simplified PDE, with a limited set of associated matrices in parts of the domain. This process is equivalent to a *downsizing of the physical model*, thus adapting it to the relevant processes.

When employing the model-adaptive methods, it is important to note that the system of linear equations does not degenerate by neglecting terms of the PDEs, because only terms that do not have an impact on the PDE are neglected. For the saturation PDE this can result in a system that is only determined by the mass-lumped storage matrix, thus only the diagonal of the linear equation system is filled.

### Caching of system matrices

Due to the non-linear coupling, the matrices mentioned previously are rebuilt in each iterative step. As the physical model was already adapted by ignoring irrelevant parts of the PDE, the regarded PDE is now spatially differing. This is not problematic, as the primary variable will stay continuous over the whole domain. During the simulation some of those matrices have to be rebuilt, others are static. E.g., in the saturated zone the capillary pressure can be neglected and the relative permeability can be assumed to be constant. In a zone of brackish water, the density changes due to salt transport. Therefore, in some parts of the system the resulting matrices can be regarded as constant, some matrices have to be rebuilt due to changes of the density. In unsaturated soil areas the flux matrices for gas and water have to be rebuilt. Furthermore, the capillary pressure vectors must be refreshed. In an area with three-phase flow multiple matrices must be recomputed.

The necessity for a rebuild is checked during a time step or iterative step. Thus the old system matrices are *cached* if possible.

The simulator has to store the matrices together with characteristic values (e.g. relative permeabilities, densities etc.), which have determined the situation in which these matrices were built. These characteristic values are evaluated during the runtime and only if the differences diverge over a critical limit, the matrices will be triggered for a recomputation. Small changes of phase mobilities, densities or velocities can be neglected, if they are below a user specified threshold. The stored matrices for flow and transport can be reused in this case.

| Reference variable of phase $\alpha$ | Matrices, Vectors |
|---|---|
| Saturation | $\mathbf{A}_\alpha$, $\mathbf{p}_{c_{0,\alpha}}$ |
| Density (function of pressures, concentrations and temperatures) | $\mathbf{A}_\alpha$, $\mathbf{C}_\alpha$, $\mathbf{D}_\alpha$ |
| Mobility (function of saturations, viscosity and for non-linear flow regimes the velocity) | $\mathbf{C}_\alpha$, $\mathbf{D}_\alpha$ |

***Table 1*** *Dependencies for matrix recalculations in the flow model.*

## EXPERIMENTAL SET-UP

A laboratory experiment was set-up in order to validate the numerical model. Its aim was to evaluate the flow behaviour under combined influence of partial saturation and density driven flow. Further details are given in *Thorenz et al.* (2002). It employed a perspex flow cell with internal dimensions of 0.958 m (length) x 0.478 m (height) x 0.105 m (width). It was equipped with two perforated sidewalls so that an inner length of 0.865 m remained. Sixteen tubes of 1 mm inner diameter were placed horizontally throughout the system to allow for tracer injection and sample extraction (Figure 1). Each of the tubes was closed at one end, perforated along a length of 10 cm and bent upwards at an angle of 90 degrees. Thus a relatively equal injection over the system thickness could be achieved and, together with the symmetry arising from the impermeable front and back plate, the system can be simplified to a 2-D system for the numerical investigations.

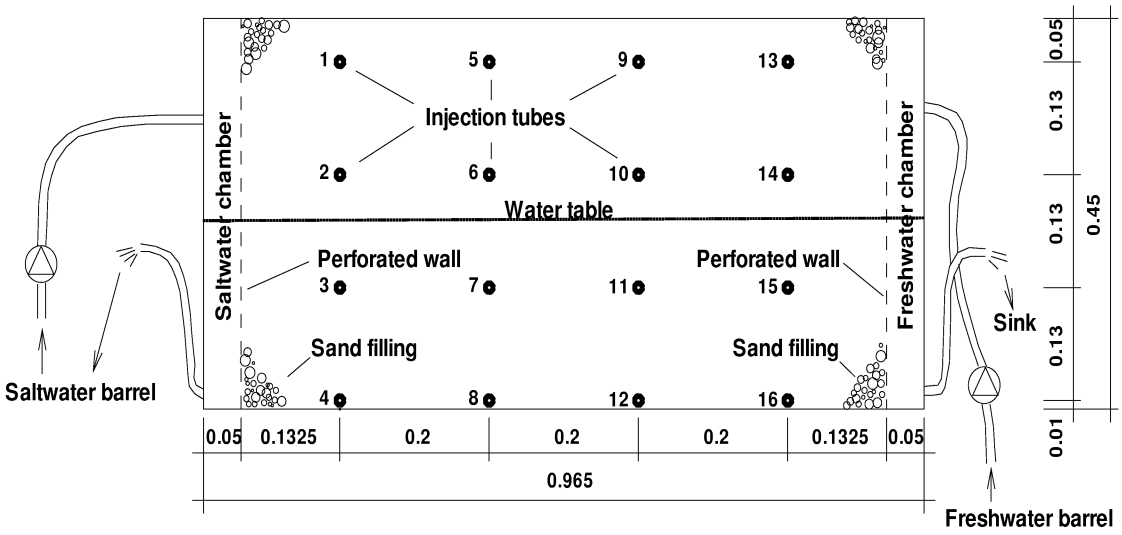


***Figure 1*** *Geometry of the sandbox.*

The filling material was a clean, natural, silica sand. The 16 sampling/injection tubes were emplaced during this packing process. To minimize hysteresis effects, the flow cell was then run through multiple imbibition-drainage cycles. Finally, the sand was covered to avoid evaporation across the upper boundary, to mimic a system at greater depth. The porosity of the sand was measured to be 0.36. The intrinsic permeability of the sand was estimated to be about $4.7 \times 10^{-11}$ $m^2$, by measuring the flux for a small gradient under saturated conditions. Samples of the sand at different heights above the fixed water table were taken to measure the water content.

Constant head boundary conditions were maintained for the experiments by filling the intake chambers of the flow cell with constant flux (100 ml/min) peristaltic pumps and using an overflow system. Regular tap water was used for all of the experiments; the barrels served as buffers to homogenize possible changes in the properties of the water (density of the freshwater was measured to be 1.067 $kg/m^3$). An electrical conductivity meter was attached to the saltwater intake as an on-line monitor of the salinity (density of the saltwater was measured to be 1.097 $kg/m^3$). After adjusting the density once, the reference conductivity was used as a standard for further adjustments.

Tracer injections (red dye) were used to visualize the flow pattern. The dye was tested against a chloride tracer and showed no measurable retardation. During the experiments time-lapse pictures of the tracer movement were taken with a programmable digital still camera.

## Experiments

In an *a priori* investigation of the flow system, using the numerical model described before, five principal flow patterns were identified, depending on the water table heights (boundary conditions) at the two sides of the system. Prescribing the saltwater and freshwater inlet chambers as being on the left and right sides of the flow cell, three experimental set-ups where identified from these as typical for the system behaviour:

- Set-up A: The pressure is uniform at the bottom on both sides of the flow cell.
- Set-up B: An intermediate state between Set-up A and Set-up C.
- Set-up C: The water table is uniform on both sides of the flow cell.

The experiments were conducted after approximately steady state conditions were reached. From the observed tracer movement pathlines were extracted in order to compare laboratory and numerical results. Figure 2 shows the results for the regarded cases. Obviously, numerical and laboratory results match very well.

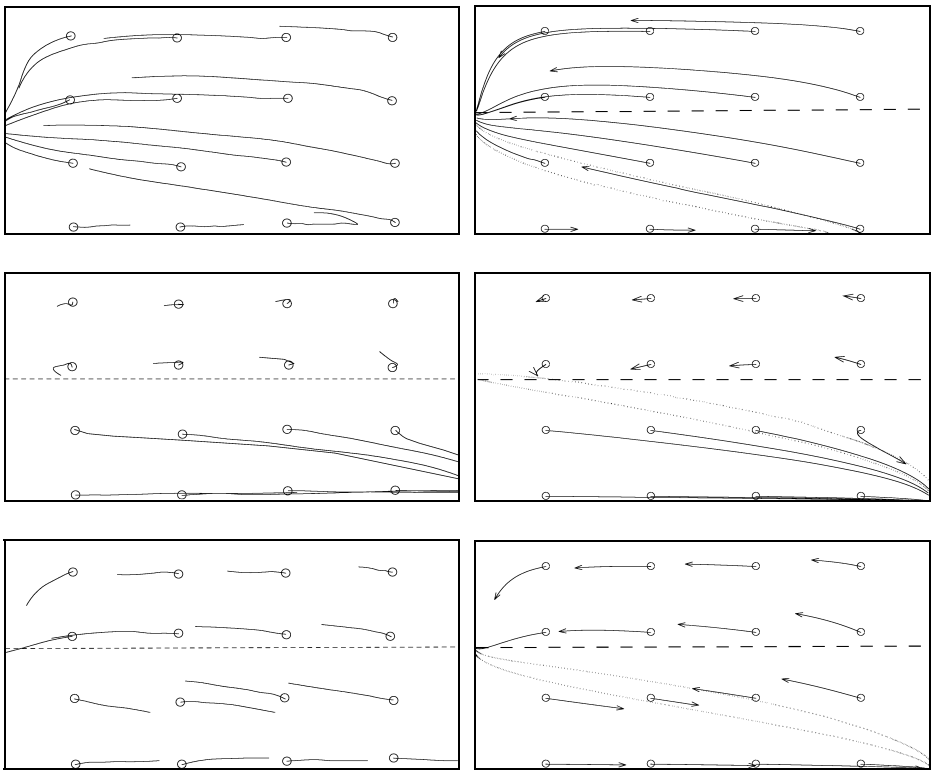

***Figure 2*** *Experimental (left pictures) and numerical (right pictures) results showing pathlines extracted from tracer movement. The location of the water table is marked by a dashed line. The dotted isoconcentration lines show computed 10% and 90% isosalinities.*

## Impact of model and grid adaptivity on execution time and accuracy

While all of the calculations presented before are performed in a steady state flow field, here the transient behaviour in the beginning of the experiment for set-up A is chosen to determine the efficiency of the model adaptive approach. This is the more difficult test case, as the transient flow field undergoes severe changes during the simulation.

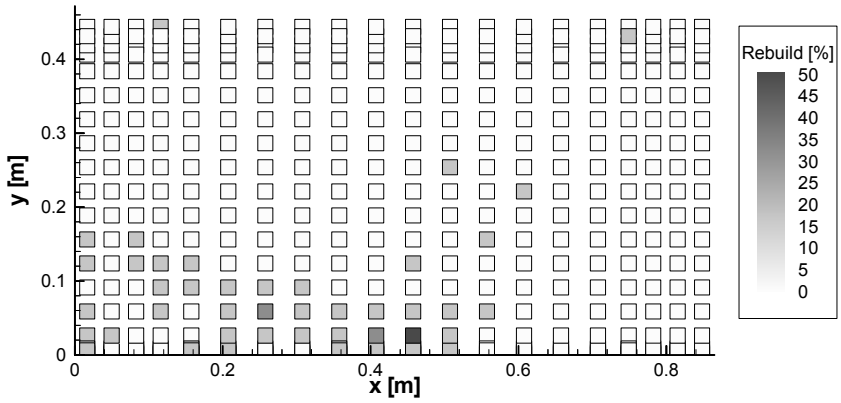


***Figure 3*** *Distribution of performed matrix recalculations for a single time step, relative to the number of recalculations for the standard approach. Mainly matrices near the head of the saltwater front are recalculated.*

In Figure 3 the percentage of performed matrix recalculations in the current time step is presented. This is the situation after 80000 seconds of saltwater intrusion. The system is not yet in steady state, as can be seen from the number of matrix recalculations around the position of the saltwater tongue. In the plot the recalculations of all matrix types are incorporated by using an arithmetic mean, they are

not weighted with the effort to build them. Obviously the unsaturated zone is already in state, as the number of recalculations is very low. In the saturated zone the recalculations concentrate on the area around the advancing saltwater tongue.

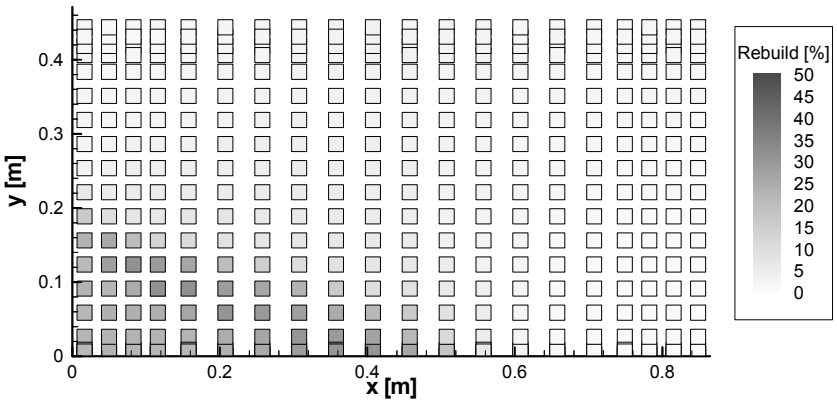


***Figure 4*** *Distribution of accumulated matrix recalculations for all time steps, relative to the number of recalculations for the standard approach.*

An additional possibility to evaluate the results is presented in Figure 4. In this plot the effort for rebuilding the system matrices was additionally averaged over all previous time steps. It becomes obvious that the computational effort is successfully focused onto the system areas where large changes of the non-linear regime took place. For the example presented above, the total computational effort is halved in comparison to the standard approach.

In order to compare the influence of both model and grid adaptivity on the results, the calculations for one of the set-ups are repeated. Two different grid resolutions are regarded in order to evaluate the influence of different grid resolutions on the computation time and the accuracy. The coarse grid is obtained by applying four bisections on the original grid, thus resulting in 6400 elements. Equivalently four bisections of the original grid are allowed in the grid adaptive scheme, too. The fine grid consists of 25600 elements and is obtained after applying five bisections.

For the fine grid all methods produced virtually equal results. In contrast, the computations on the coarse grid showed significant differences. The grid adaptive method suffers from numerical dispersion problems, while the standard approach can produce fair results even though a rather coarse grid is used. Even more astonishing is a comparison of the computation times (Table 2). The grid adaptive approach uses even more computation time than the standard approach. A closer look on the performance data during the simulation reveals that the simulator has to more non-linear iterations in each time step, because the grid adaptation has disturbed the previous equilibrium of the flow field. The model adaptive approach produces results that are indistinguishable from the standard approach, while significantly reducing the computation time. For the model adaptive and the standard approach the coarse grid results are already very close to the results on the finer grid, while the grid adaptive scheme requires further refinement of the grid.

| Modelling approach | CPU-time (fine grid) | CPU-time (coarse grid) |
|---|---|---|
| Standard approach | 100% | 100% |
| Grid adaptive approach | 110% | 106% |
| Model adaptive approach | 54% | 51% |

***Table 2*** *Comparison of computation time for the standard, grid adaptive and model adaptive approaches.*

It must be stressed that these results cannot be generalized. For finer meshes the results of the grid adaptive scheme are very good. Furthermore, the amount of needed computer memory is largely reduced with the grid adaptive approach.

### Conclusions

The laboratory experiments discussed here demonstrate clearly that a significant lateral flow, and coupled density-driven flow effects, take place in the partially saturated region above the water table, and at the interface between the saturated and partially saturated zones. The flow behaviour is complex and may show unexpected behaviour. Although it is difficult to extrapolate these small-scale experiments to the field scale, similar flow behaviours can be expected at the saltwater/freshwater interface in unconfined aquifers.

The model adaptive approach was tested in terms of accuracy and speed against the standard procedure. The results are rather promising, as a substantial increase in execution speed was observed. In this case the accuracy degradation was so small that no differences to the standard method could be observed. Further acceleration can be expected by using less accurate matrix re-evaluation criteria, but in this case accuracy will suffer.

## REFERENCES

Bear, J., Dynamics of Fluids in Porous Media, Elsevier, New York, 1972

Busch, K.-F., L. Luckner and K. Tiemer, Lehrbuch der Geohydraulik, Band 3, Geohydraulik, Gebrüder Bornträger, Berlin, Stuttgart 1993

Kolditz, O., R. Kaiser, D. Habbar, T. Rother, and C. Thorenz, RockFlow/RockMech- Theory and Users Manual, Release 3.6, Groundwater Modelling Group, Institute for Fluid Mechanics and Computer Application in Civil Engineering, Univ. Hannover, 2001

Sahimi, M., Flow and Transport in Porous Media and Fractured Rock, VCH-Verlagsgesellschaft, Weinheim, New York, Basel, Cambridge, Tokyo, 1995

Scheidegger, A. E., General Theory of Dispersion in Porous Media, Journal of Geophysical Research, Vol. 66, No. 10, 1961

Thorenz, C., Model Adaptive Simulation of Multiphase and Density Driven Flow in Fractured and Porous Media, Dissertation, Institute for Fluid Mechanics and Computer Application in Civil Engineering, Univ. Hannover, 2001

Thorenz, C., G. Kosakowski, O. Kolditz and B. Berkowitz, An experimental and numerical investigation of saltwater movement in coupled saturated/partially-saturated systems, Water Resources Research, 2002, in press